MEDDOCS
Open Access Publisher

ISSN: 2640-1193

Journal of Tuberculosis

Open Access | Research Article

Cellular trafficking of nanocarriers in alveolar macrophages for effective management of pulmonary tuberculosis

Vipul A Sansare*; Deepa U Warrier; Ujwala A Shinde

Department of Pharmaceutics, Bombay College of Pharmacy, Kalina, Santacruz (E), Mumbai, 400098

***Corresponding Author(s): Sansare VA**
Department of Pharmaceutics, Bombay College of Pharmacy, Kalina, Santacruz (E), Mumbai, 400098
Tel: 869293076; Email: avipulsansare@gmail.com

Received: Mar 05, 2020

Accepted: Apr 17, 2020

Published Online: Apr 21, 2020

Journal: Journal of Tuberculosis

Publisher: MedDocs Publishers LLC

Online edition: http://meddocsonline.org/

Keywords: Pulmonary tuberculosis; Rifampicin; Inhalable nanostructured lipid carriers; Mannose conjugation; Macrophages selective drug delivery.

Abstract

The aim of the present study was to design mannose anchored rifampicin nanostructured lipid carrier for active targeted drug delivery to alveolar macrophages. Targeting ligand, N-octadecyl-mannopyranosylamine was synthesized and characterized. Rifampicin loaded nanostructured lipid carriers were composed of stearic acid, oleic acid and targeting ligand and were prepared by melt homogenization ultrasonication. The N-octadecyl-mannopyranosylamine decorated rifampicin loaded nanostructured lipid carriers were further characterized for physical state of component, *In-vitro* release, *in-vitro* lung deposition, drug loading as well as drug antimicrobial activity on *Bacillus subtilis* strain. Moreover cytotoxicity and cell internalization ability were evaluated on alveolar macrophages RAW 264.7 cell lines by confocal laser scanning microscopy. The nanostructured lipid carriers exhibited good aerodynamic characteristics and sustained drug release profile with preserved antimicrobial activity. The studies on cell lines demonstrated non-cytotoxicity of nanocarriers. The mannose anchored nanocarriers were found to internalize efficiently in cell cytoplasm than unconjugated nanocarriers. The prepared alveolar macrophages targeted rifampicin loaded nanostructured lipid carrier exhibited suitable features for inhaled therapy and could be considered as a promising avenue for tuberculosis therapy by means of a dry powder inhaler device.

Introduction

Tuberculosis (TB) has remained, unambiguously, a significant health care problem since long times, particularly in developing and under developed countries. The chemotherapy for the treatment of TB is extremely difficult due to the long treatment period and patient noncompliance, leading frequently to the emergence of Multidrug Resistant (MDR) strains [1]. The therapy becomes more complicated and compromised with the emergence of HIV/AIDS pandemic [2]. In this context, new and improved drug delivery strategies for existing drugs may play a crucial role in the TB management [3,4]. Targeted and sustained release chemotherapy offers a great potential in tuberculosis treatment by achieving greater specificity of delivery and improved therapy [5]. Because *M. tuberculosis* is known to infect alveolar macrophages (AMs) and affect the pathogenesis of tuberculosis, there have been renewed interests in targeting of anti- tuberculosis drugs to these cells [6].

The etiological agent of TB is located in the AMs, more specifically inside the acidic compartments of the phagosomes and phagolysosomes. The infected macrophages have been reported to overexpress certain receptors, which can efficiently be targeted with appropriate drug delivery systems [7].

Cite this article: Sansare VA, Warrier DU, Shinde UA, Cellular trafficking of nanocarriers in alveolar macrophages for effective management of pulmonary tuberculosis. 2020; 3(1): 1016.

AMs are pivotal regulators of immunological homeostasis and key effector cells in first line host defence. Intracellular location of bacteria protects them from host defence mechanisms and restricts penetration of antibiotics [8]. It is, therefore, necessary to maximize drug uptake by AMs for efficient sterilization of microbial load. Once targeted, cells themselves could serve as a vehicle from where drug would be released from carrier system. However, inadequate specificity for macrophages and poor internalization potential of carriers constitute critical obstacles to success of such delivery systems. TB infection leads to AMs activation which over express mannose (MR-CD 206 and CD 163) [9,10] receptors. Such activated macrophages can recognize and facilitate internalization of carriers bearing mannosylated carbohydrate molecules [11,12]. Therefore an effort has been directed towards development of ligand-decorated carrier systems for cell-selective targeting. Such carriers are efficiently phagocytised by AMs and deliver high payload of drug [13]. Nanotechnology platforms are currently being explored for sustained delivery anti TB drugs to lungs. SLN has emerged as promising nanocarriers with superior physicochemical characteristics viz. small size, biocompatibility and deep-lung deposition ability [14]. Dual effect of prolonged drug release and rapid drug transport could be achieved by means of SLNs [15]. Local delivery to lungs by inhalation has become one of the most attractive administration routes to target TB infection's cellular reservoir, while reducing systemic adverse effects [16,17]. Lipids used in fabrication of SLNs are biodegradable, non-immunogenic; whose functionality can be easily modified and hence enhancing tendency of phagocytic uptake by macrophage cells [18]. The benefits of inhalable lectin-targeted carriers could lead to greater patient compliance and curtail the emergence of drug-resistant *M. tuberculosis* strains.

Lipid-based particulate systems for TB inhaled therapy have been investigated less deeply though they were generally recognized as safe, non-swellable upon contact with the lung moisture and, consequently, able to retain the embedded drug before the target site. Among the lipid-based particulatesystems, most of the studies have focused on liposomes [19-24] whereas less attention has been paid to the solid lipid particles [25,26] although their advantages over liposomes in terms of physical stability. Solid Lipid Microparticles (SLM), constituted by a solid lipid core stabilized bya surfactant at the surface, represents an advantageous approach to improve TB management. SLM exhibited several favourable properties as production without organic solvents, high drug loading levels and long-term stability. Furthermore, they could be considered proper to provide values of aerodynamic diameter essential for the particle deposition in the deep lung [27].

Various studies have shown that the mannose receptors have high affinity for carbohydrates, are specifically expressed by activated macrophages in tuberculosis infection.Therefore, drug loaded particulates conjugated to carbohydrate can ensure targeting and internalization of drug by lectin positive macrophages in pulmonary tuberculosis [11,28]. After internalization of these particulates, release of the drug in sustained manner helps in achieving improved therapeutic benefits with lower doses. Lipid particulate carriers are one of the antimicrobial drug delivery platforms that have attracted much attention currently. Lipid particulates can provide a sustained release of the carried antimicrobial payloads, which can effectively eliminate the infectious microbes harbored at the lymphatic sites. Moreover, currently the pulmonary drug delivery is the preferred route of administration of aerosolized drugs in the treatment of pulmonary TB, delivering the drug directly to the site of infection through inhalation of an aerosolized delivery. On the basis of aforementioned key points the present project envisaged the development of novel lipid particulate formulation in which carbohydrate anchored lipid particulates loaded with Rifampicin (RIF) for targeted and sustained delivery via pulmonary route with reduced systemic side toxicities and improved patient compliance.

Material and methods

Material

Rifampicin was kindly gifted by Lupin Ltd, India. Soya lecithin S-100 was gifted by Lipoid, Germany. Stearic acid was purchased from Loba Chem. ltd., India. Tween 20, D-mannose, mannitol, L-leucine and oleic acid were purchased from S.D. Fine-Chem Ltd. India. Stearylamine was purchased from TCI Chem. Pvt. Ltd. India. Nutrient agar and nutrient broth were purchased from Himedia, India. Nile red was purchased from Sigma Aldrich India. Alveolar macrophage cell line (RAW 264.7) was purchased from National center for cell science, India. All other regents and chemicals were purchased locally.

Synthesis and characterization of N-octadecyl-mannopyranosylamine

Synthesis was carried out by method as reported by Witoonsaridsilp W et al [29]. with slight modification. Briefly, a 5 mM of stearylamine was dissolved in 15 ml ethanol and heated up to 70˚C, after which 5 mM of D-mannose was added with continuous stirring (200 rpm). This solution was stirred for 15 min till mannose was completely dissolved. The solution was cooled to 40˚C and diluted with 35ml n-hexane. The reaction was monitored with thin layer chromatography. Hexane: Ethyl acetate (8:2) was used as mobile phase and spots were detected in presence of UV light. The obtained crystals were collected at room temperature and characterized by FTIR, Mass and NMR spectroscopy.

Preparation of RIF NLCs

RIF NLCs were prepared by melt homogenization ultrasonication method [30]. In practice RIF (25mg) was dissolved in stearic acid: oleic acid (500 mg) and melted at 70˚C. 0.25 % w/v soya lecithin S-100 (25 mg) was transferred in melted lipid. Aqueous surfactant solution containing 10 ml of distilled water and 1.5% w/v of Tween 20 was injected using syringe (21 gauge) into molten lipid mass and stirred at 4000 rpm for 10 minutes at 70˚C using overhead stirrer (Remi, India).The obtained pre emulsion was subjected to probe sonication (VCX500, Sonics and materials, U.S.A.) at 20% amplitude for 10 minutes and cooled to room temperature. For further particle size reduction, the NLC dispersion was subjected to homogenization using high pressure homogenizer (Stansted, UK) at 20,000 psi for 3 cycles. Mannose conjugated RIF NLCs prepared by NODM addition in molten lipid mass (10% w/w of total lipid). NLCs were labelled with nile red (0.001% w/v) for cellular uptake studies.

Particle size, zeta potential and entrapment efficiency determination

Particle size and zeta potential of RIF NLCs were determined with the aid of photon correlation spectroscopy (Zetasizer Nano ZS, Malvern Instruments, Worcestershire, UK) at 25°C. Sample was appropriately diluted with distilled water to prevent interparticle scattering. The percentage entrapment efficiency of RIF in the RIF loaded NLC dispersions was determined using the in-

direct method. The RIF loaded NLC dispersions were subjected to ultra-centrifugation at 80,000 rpm for 1h at 4°C using Optima Max XP ultracentrifuge (Beckman Coulter, U.S.A.) to separate the unentrapped drug. Supernatant was diluted and analyzed by UV spectrophotometry at λ_{max} of 337 nm using methanol AR as blank for quantification of unentrapped or free RIF. Percentage entrapment efficiency was calculated by using equation 1.

Percent entrapment efficiency= (WL-WF) × 100 ÷ WL…….. (1)

Development of RIF loaded NLCs based DPI

Mannitol was used as carrier for pulmonary delivery of NLCs. NLC dispersion was mixed with mannitol at 1:2 total lipid to mannitol ratio. L-leucine (1%w/v) was added as anti-adherent and the resulting NLCs dispersion was spray dried using spray drier (Labultima-222, India) [31].

Particle size and morphology

Particle size of spray dried NLCs was investigated using Malvern Zetasizer Nano ZS at 25°C. The morphology of the spray dray dried NLCs was viewed by means of scanning electron microscopy (SEM) (Philips XL 30, Japan). The SEM samples were loaded on aluminium stub with carbon adhesive tape and gold was applied for electron conductivity. Samples were scanned at a voltage 10kV and the images were taken.

Assay of RIF in spray dry powder

Spray dried NLCs equivalent to 3mg of RIF (369.23mg) was dissolved in 100 ml of methanol AR and maintained in darkness for 24 h at room temperature; subsequently the solution was subjected to bath sonicator. The concentration of RIF was measured spectrophotometrically at 337 nm wavelength. (V-530, Jasco, Japan). Finally the percentage of RIF in spray dried NLCs were compared to initial value and the percentage of RIF entrapped in the spray dried NLCs was calculated. The value considered was average of three determinations.

***In-vitro* release study**

RIF release from NLCs and RIF solution were examined on weighed samples using dialysis diffusion technique at 37±0.5°C and quantification was carried out by spectrophotometric method. Briefly, 3mg of RIF and equivalent of RIF NLCs were separately dispersed in 4 ml of simulated lung fluid (SLF) pH 7.4. The resulting dispersion was added to dialysis bag (MWCO 13000-14000 Da, Himedia, India) and was dialyzed separately against 150 ml of SLF (pH 7.4). At predetermined intervals, 5ml aliquots were withdrawn filtered through 0.45 µm membrane filter and RIF content was determined spectrophotometrically. The release medium was replenished with an equal volume of fresh SLF maintained at same temperature. Each experiment was performed in triplicate and the mean value of percent cumulative release and standard deviation at each time point were calculated.

***In-vitro* lung deposition of spray dried NLCs**

Lung deposition of spray dried NLCs was assessed using Andersen Cascade impactor (ACI) (Cooply Scientific). NLCs equivalent to 0.3 mg of RIF was filled in each HPMC capsule size 3 (ACG, India). The flow rate was maintained to 60 ± 5 L/min. The spray dried NLCs in each capsule were aerosolized for 10 seconds using inhaler device (Lupihaler®). Methanol AR was used to rinse particles deposited on each stage and RIF content was determined spectrophotometrically. The mass median aerodynamic diameter (MMAD), % fine particle fraction (FPF), fine particle dose (FPD) were calculated from the percentage of RIF propelled from delivery device.

Differential scanning calorimetry (DSC) of RIF NLCs and components

Thermograms of RIF, stearic acid, stearic acid: oleic acid (8:2), mannitol, RIF NLCs and NODM conjugated RIF NLCs were recorded by DSC (Perkin-Elmer Pyris 1, USA) in order to investigate the effect of formulation process on the physical state of the components. The samples were heated from 30°C to 300°C at a heating rate of 10°C/min with nitrogen purging (20 mL/min) and endotherms were recorded.

Antimicrobial activity

In-vitro antibacterial activity study of RIF NLCs was performed using agar well diffusion technique to investigate whether RIF activity was maintained in the lipid particles. Nutrient broth and *Bacillus subtilis (B.subtilis)* ATCC 6633 were used as growth medium and microorganism strain respectively. The wells in agar plate were filled with 100µl of sterile RIF solution as reference. Each solution was serially diluted (two folds) to construct the calibration curve by relating inhibition zone diameter to RIF concentration of standard solution. Other well in agar plate was filled with RIF NLCs (10 ppm) dissolved in methanol. The plates were incubated at 37 ± 2°C and inhibition zone diameter was measured. The inhibition zone diameter produced by the RIF NLCs was plotted on the calibration curve to calculate concentration of RIF in RIF NLCs.

***In-vitro* cytotoxicity study**

RAW 264.7 cell lines were seeded in 96 well plate at density $1*10^4$ cells in 100 µl of Dulbecco's modified Eagle's Medium (DMEM) high glucose with 10 % Fasting blood sugar (FBS) medium. The plates were incubated in anaerobic condition with 5 % CO_2 at 37 °C for 48 h to obtained complete monolayer. Cells were then incubated with serial dilutions (1, 10, 50, 100 µM) of samples (RIF, unloaded NLCs, RIF NLCs, NODM conjugated RIF NLCs), medium as negative control and dimethyl suphoxide as positive control for 37 °C, 5% CO_2 for 48h. After incubation times, the methyl thiazole tetrazolium test (MTT) was performed as per procedure described in [32]. The results were expressed as percentage of cell viability.

Cell internalization study

The samples (unconjugated NLCs and mannose conjugated NLCs) were suspended in phosphate buffer (PBS) and diluted using DMEM to a final NLC amount of 0.25mg/ml. RAW 264.7 cells were plated in 6-well plates (300,000 cells/well) and incubated for 12 h with the sample suspension at 37°C. After 12 h incubation, cells were washed with PBS and observed by confocal laser scanning microscopy (DMIRE2, Leica Microsystems GmbH, Wetzlar, Germany) [27].

Results and discussion

Synthesis and characterization of NODM

FTIR spectrum of D-Mannose, stearylamine and synthesized (NODM) were recorded and shown in Figure 1. In spectrum of D-Mannose, broad peak at 3398 cm^{-1} and intense peak at 2926 cm^{-1} indicate the presence of –OH stretching and $–CH_2$ stretching vibrations. Vibrational signals at 1064 and 1638 cm^{-1} indicate C=O stretching of either alcohol or aldehyde groups in mannose.

In the spectrum of stearylamine, sharp lower intensity peak at 3331 cm^{-1} indicate $–NH_2$ stretching of primary amine group of stearylamine. Vibrational signals at 2917 and 2849 cm^{-1}indicate $–CH_2$ stretching of long alkyl chain. These two peaks were found to be more intense than that of mannose due to presence of long alkyl chain in stearylamine. Vibrational peaks at 1606 and 1471 cm^{-1} indicate presence of $–NH_2$ and $–CH_2$ bending. Spectrum of NODM showed lower intensity peak at 3383 cm^{-1}. This is due to combination of $–NH_2$ stretching of stearylamine and –OH stretching of mannose. Peak at 1606 cm^{-1} observed in stearylamine appear at lower intensity in NODM, indicating the conversion of primary amine (stearylamine) to secondary amine (NODM). Reduced intensity of peaks at 1606 cm^{-1} and 3383 cm^{-1} indicates the secondary amine linkage between mannose and stearylamine.

NMR and mass spectrum of synthesized NODM is shown in Figure 2 & 3 respectively. In proton NMR spectrum, presence of lower intensity -NH proton signal at 2.7 ppm indicates the secondary amine linkage between mannose and stearylamine. In mass spectrum, M^{+1} peak at 432.4 indicates the presence of desired compound, since the molecular weight of NODM was 431.

Preparation and evaluation of RIF NLCs

NLCs loaded with RIF were developed in perspective of a pulmonary therapy of tuberculosis with an objective to investigate the suitability of lipid carrier to target the RIF inside the alveolar macrophages. A major advantage of these lipid particles as drug carrier is related to the biocompatibility and preparation technique that avoids organic solvents. The particle size and zeta potential of prepared NODM conjugated NLCs were found to be 240.9 nm (PDI: 0.135) and -43.3 mV. High negative value of zeta potential indicates formation of stable NLC dispersion. It was found that RIF could be entrapped with relative high efficiencies in NLCs dispersion (52±0.88 %.) due to careful selection of lipids and surfactants as well as partial lipophilic nature of RIF.

Development and characterization of RIF loaded NLCs based DPI

Physical properties of spray dried RIF NLCs

Particle size of spray dried RIF NLCs was found to be 409.5 nm with PDI 0.324 which indicates, NLCs are able to redisperse in water after dissolution of carrier. The NLCs dispersion showed particle size of 240.9 nm and after spray drying, particle size of NLCs was 409.5 nm; the increase in particle size after spray drying could be due to melting and aggregation of lipid matrix during spray drying.

SEM photomicrographs of RIF and RIF NLCs are shown in Figure 4a & 4b. RIF is reported to be crystalline, rod shaped crystals. This was evident from the SEM image of RIF which showed clear elongated crystals ranging from 10-20 µm in size. The spray dried NLCs were observed to be nearly spherical in shape and smooth surface which is suitable for lung delivery. Moreover, the entrapment of RIF did not modify the NLCs morphology.

The physical state of NLCs were evaluated by DSC and compared with those of corresponding components (Figure. 5). RIF, stearic acid and mannitol displayed sharp endothermic peaks at 196.8°C, 63.2°C and 172.3°C due to their melting [33,34]. Furthermore, the endothermic peak for the mixture of stearic acid and oleic acid was shifted to 55.5°C and with lesser intensity than that for pure stearic acid. This indicates reduction in crystallinity of the lipid, which may be attributed to the formation of liquid lipid pockets within the solid lipid. The thermograms of RIF loaded NLCs displayed the presence of diminished and broad peaks of stearic acid and mannitol **(**Figure 5b) [33]. This was due to a transition of crystalline to amorphous state in the NLCs. The absence of sharp endothermic peaks related to the stearic acid in the DSC thermograms confirmed this hypothesis. This will possibly minimize the RIF expulsion form the lipid matrix facilitates the drug retention in the lipid matrix.

***In-vitro* release study**

In-vitro drug release study is a measurement of release of Active Pharmaceutical Ingredient (API) from the formulation matrix, is important evaluation parameter for product development and quality control. In present study *in-vitro* release study of spray dried RIF NLCs was performed using dialysis tube diffusion technique by using dissolution apparatus. All studies were performed in triplicate and results are expressed in mean ± SD. Percent cumulative release of RIF from RIF solution and spray dried RIF NLCs is graphically represented in Figure 6.

Spray dried RIF NLCs show sustained release profile up to 96 h whereas RIF solution showed 10 h release profile. This could be due to poor wettability of lipid nanocarriers particles and high lipid solubility of RIF. Similar result was reported by [35,36], where RIF release from RIF lipid microparticle showed sustained release profile in SLF pH 7.4 over a period of 100 h.

***In-vitro* lung deposition of spray dried NLCs**

ACI separates a sample into fractions based on inertia, which is a function of particle density, shape and velocity. Three important parameters determined from ACI study are MMAD, geometric standard deviation (GSD), FPF less than 5 µm [37]. FPF indicates respirable fraction and it is a fraction of total inhaled drug that reaches the stage corresponding to cut off diameter of 5 µm. *In- vitro* lung deposition studies of spray dried RIF NLCs was performed using ACI. The amount of drug deposited on each stage was calculated and represented in Figure 7.

Based on drug deposited on device, capsule and stages of ACI, Recovered Dose (RD), Emitted Dose (ED), FPD, FPF, MMAD and GSD were calculated. MMAD of spray dried formulation was 4.71, which is suitable for lung deposition. Approximately 34% of drug was deposited in the preseparator and induction port. This may be due to particle aggregation in presence of humidity. Higher emitted dose indicates good flow properties of powder.

Antimicrobial activity

The microbiological assay was performed on RIF NLCs dissolved in methanol: water mixture. Methanol was selected for complete extraction of RIF from NLCs without reducing biological activity. The *B. subtilis* ATCC 6633 strain was chosen because of its susceptibility to RIF [38,39]. The zone of inhibition provided by dissolved NLCs was compared with those produced by standard RIF solution (Figure 8). NLCs produced inhibition zone diameter corresponding to the RIF loading value (5 ppm), thus providing evidence of antimicrobial activity preservation after entrapment of RIF in lipid matrix. The unloaded NLCs did not provide zone of inhibition indicating that lipid matrix did not interfere with the assay.

Cytotoxicity and internalization capacity by RAW 264.7 cell lines

Both cytotoxicity and capacity of NLCs to interact with alveo-

lar macrophages were studied by means of macrophages RAW 264.7 cell lines. RIF loading level was considered for the selection of sample amount. To make NLCs fluorescent, nile red was embedded into the lipid matrix. Nile red is lipid soluble dye and it is a vital stain for the detection of intracellular lipid material by confocal laser scanning microscopy [40].

Concerning cytotoxicity of NLC samples at four different concentrations of RIF, MTT test results expressed as percent cell viability are shown in Figure 9. Rifampicin loaded NLCs exhibited a dose dependent cytotoxicity that increased with the concentration. However only negligible cytotoxicity with cell viability over 85% was found at 100 Mmol concentrations. These results are consistent with those observed for stearic acid based lipid carriers.

In order to clarify the location of NLCs in the cell, confocal microscopy was performed. The image obtained under filter set for red and blue fluorescence from the cells incubated with mannose conjugated NLCs (Figure 10) was compared with that of non-conjugated NLCs. RAW 264.7 cells incubated with mannosylated NLCs revealed the presence of marked red fluorescent spots around the respective nuclei having size corresponding to that of nanoparticles indicating presence of NLCs inside the cell cytoplasm. Conversely, a negligible or slight fluorescent spots were observed from the cells incubated with unconjugated NLCs. Concerning mechanism of cell entry, receptor mediated endocytosis is established for efficient entry of mannosylated NLCs over unconjugated NLCs.

Due to lipophilic nature of RIF that is able to retain drug within NLCs matrix, as demonstrated by the *in-vitro* release study, it could be hypothesized that RIF remains embedded within the NLCs during the uptake process. Although *release* of RIF was negligible, there could be a possibility of leakage from NLCs, inside the macrophages to exert anti-tubercular activity, as observed both *in-vivo* and *iv-vitro* by other authors [41] owning to the intracellular biodegradation of the lipid matrix. Therefore, an anti-tubercular activity inside infected alveolar macrophages can be expected.

This preliminary phase of the study is not sufficient to predict the *in-vivo* effectiveness of the lipid based system in human TB treatment. The next step of the study will consider effectiveness in infected cells and animals.

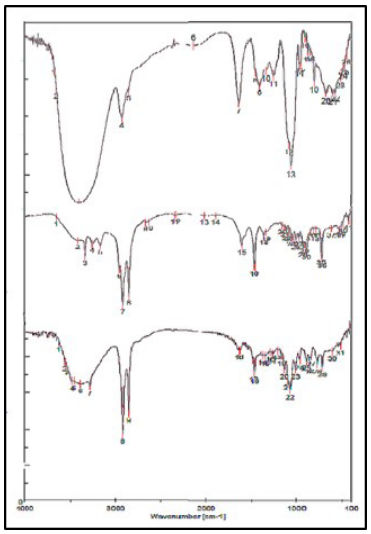

Figure 1: FTIR spectrum of D-mannose, strearylamine and NODM.

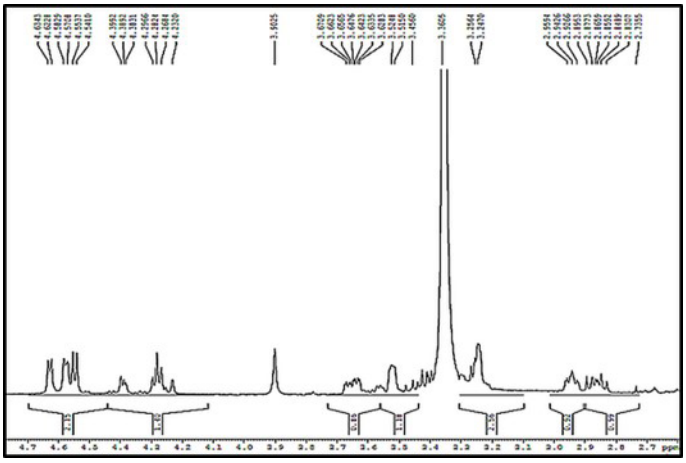

Figure 2: Proton NMR spectrum of synthesized NODM.

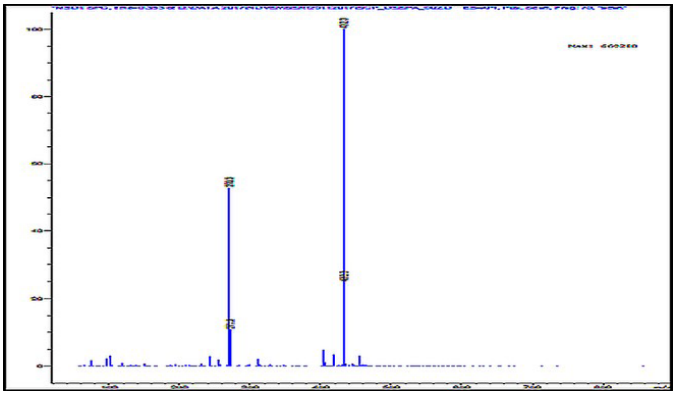

Figure 3: Mass spectrum of synthesized NODM.

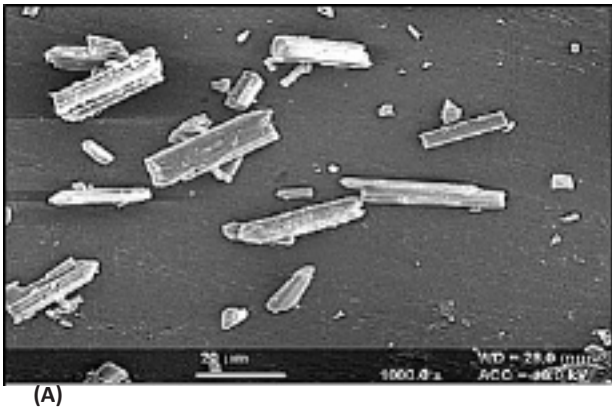

(A)

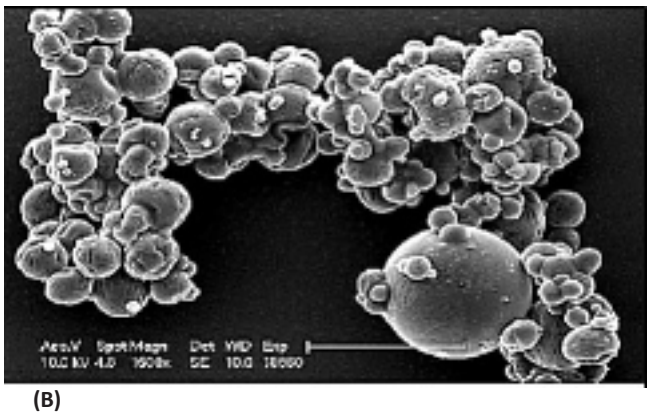

(B)

Figure 4: SEM images of a) RIF b) Spray dried RIF NLCs.

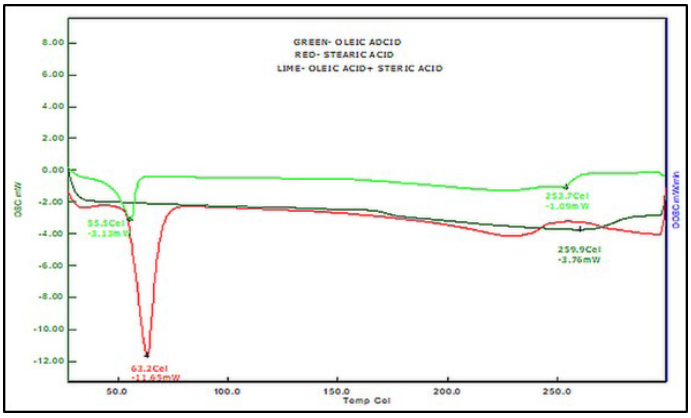

Figure 5a: DSC thermograms of oleic acid, stearic acid and physical mixture stearic and oleic acid.

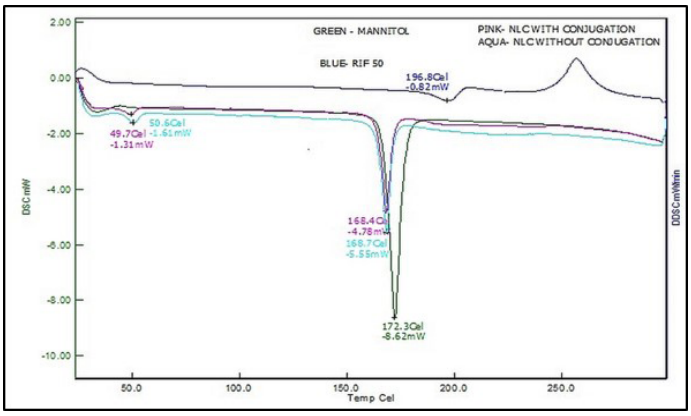

Figure 5b: DSC thermograms of oleic acid, stearic acid and physical mixture stearic and oleic acid.

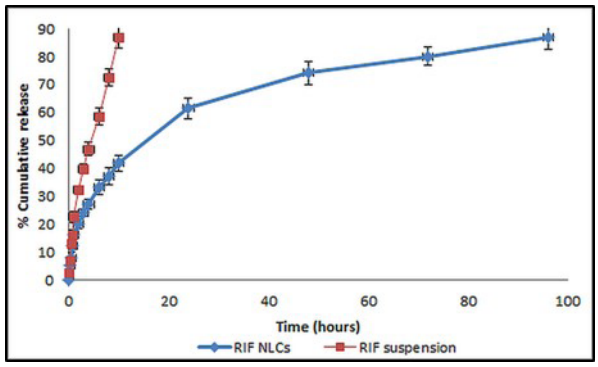

Figure 6: *In-vitro* release profile of RIF suspension and RIF NLCs

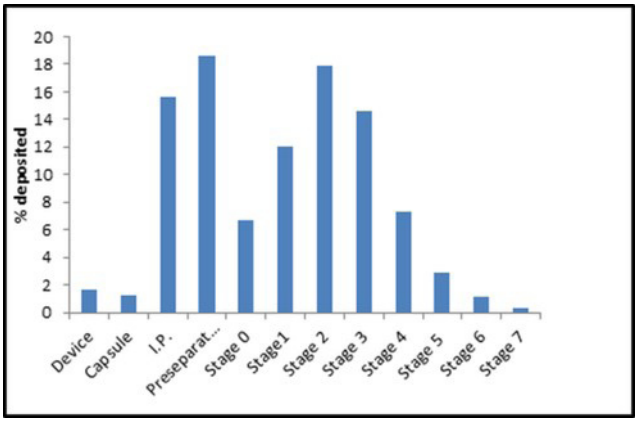

Figure 7: Comparative plot of % of drug deposited on each stage of ACI.

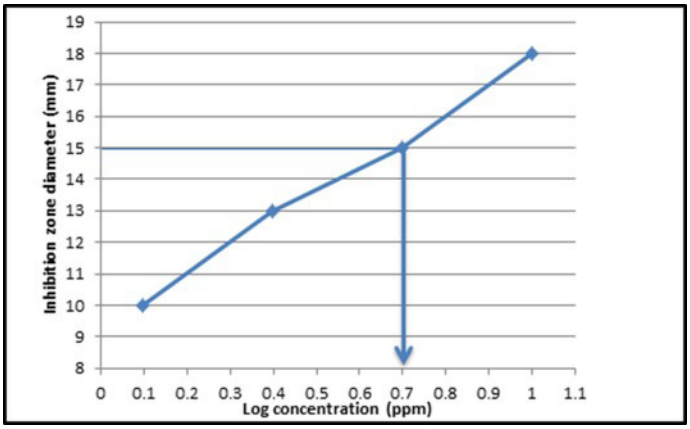

Figure 8: RIF antimicrobial activity from spray dried NLCs.

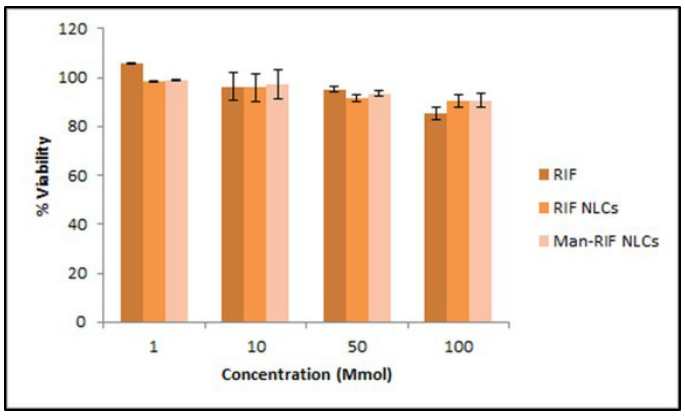

Figure 9: MTT test on RAW 264.7 cell line incubated with different concentrations of RIF, RIF NLCs and mannosylated RIF NLCs.

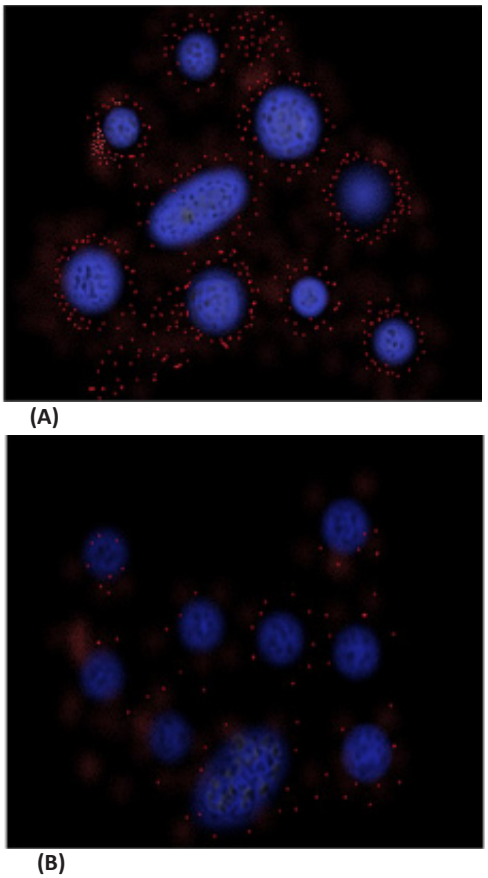

Figure 10: Confocal microscopy images of RAW 264.7 cells after nuclei staining and incubation with a) Mannosylated RIF NLCs b) Unconjugated RIF NLCs.

Conclusion

Thus aim of the present study was to develop ligand conjugated RIF loaded nanostructured lipid carrier (NLCs) based dry powder for inhalation to provide AM targeting, reduce dose related side effects and formulate an acceptable dosage form. The major outcomes of this study was the successful synthesis of mannose conjugated lipid, entrapment of RIF within a lipid core and spray drying of optimized RIF NLCs dispersion. The RIF NLCs dispersion showed good quality control parameters (particle size below 300nm, PDI 0.135). The spray dried NLCs were found to be spherical, micron size particles thus showing suitability for pulmonary administration. The spray dried formulation showed efficient release of nanoparticles after dispersion in water. The formulation also showed antibacterial activity, in terms of zone of inhibition as compared to RIF solution. However, *in-vivo* organ distribution studies are necessary to confirm distribution of NLCs inside the alveolar macrophages. Thus, the developed RIF loaded NLCs based dry powder for pulmonary drug delivery may prove to be useful in the therapy of tuberculosis.

Acknowledgements

We would like to thank Lipoid (Germany), Lupin Ltd. (India), Vav Life Science (India), Diya labs (India), Department of Nanoscience, University of Mumbai (India), Punjab University (India), Central Institute of Research on Cotton Technology (India), Ambarnath Organics (India) and Kelkar Research Center (India) for excellent technical support.

References

1. Lienhardt C, Vernon A, Raviglione MC. New drugs and new regimens for the treatment of tuberculosis: Review of the drug development pipeline and implications for national programmes. Curr Opin. 2010:186-193.
2. Blumberg HM, Burman WJ, Chaisson RE, Daley CL, Etkind SC, et al. American Thoracic Society/Centers for Disease Control and Prevention/Infectious Diseases Society of America: treatment of tuberculosis. Am J Respir Crit Care Med. 2003; 167: 603-662.
3. Costa A, Pinheiro M, Magalhães J, Rabeiro R, Seabra V, et al. The formulation of nanomedicines for treating tuberculosis . Adv Drug Deliv Rev. 2016; 102: 102-115.
4. Sung JC, Pulliam BL, Edwards DA. Nanoparticles for drug delivery to the lungs. TRENDS Biotechnol. 2007; 25: 563-570.
5. Hwang SM, Kim DD, Chung SJ, Shim CK. Delivery of o fl oxacin to the lung and alveolar macrophages via hyaluronan microspheres for the treatment of tuberculosis. J Control Release. 2008; 129: 100-106.
6. Lawlor C, Kelly C, Leary SO, sullivan MPO, Gallagher PJ, et al. Cellular targeting and traf fi cking of drug delivery systems for the prevention and treatment of MTb. Tuberculosis. 2011; 91: 93-97.
7. Cohen SB, Gern BH, Delahaye JL, Sherman DR, Gerner MY, Urdahl KB. Alveolar Macrophages Provide an Early Short Article Alveolar Macrophages Provide an Early Mycobacterium tuberculosis Niche and Initiate Dissemination. Cell Host Microbe. 2018; 24: 439-446.e4.
8. Alexandru-flaviu T, Cornel C. Macrophages Targeted Drug Delivery as a Key Therapy in Infectious Disease. Biotechnol Mol Biol Nanomedicine. 2014; 2: 19-21.
9. Ernst JD. Macrophage Receptors for Mycobacterium tuberculosis. Infect Immun. 1998; 66: 1277-1281.
10. Stahl PD, Ezekowitzt RAB. The mannose receptor is a pattern recognition receptor involved in host defense. Curr Opin Immunol. 1998; 10: 9-11.
11. Jain K, Kesharwani P, Gupta U, Jain NK. Biomaterials A review of glycosylated carriers for drug delivery. Biomaterials. 2012; 33: 4166-4186.
12. Azad AK, Schlesinger LS. Mycobacterium tuberculosis Activates Human Macrophage Peroxisome Proliferator-Activated Receptor γ Linking Mannose Receptor Recognition to Regulation of Immune Responses. J Immunol. 2011; 185: 929-942.
13. Zaki NM, Tirelli N. Gateways for the intracellular access of nanocarriers: A review of receptor-mediated endocytosis mechanisms and of strategies in receptor targeting. Expert Opin. 2010; 7: 895-913.
14. Chakraborty S, Shukla D, Mishra B, Singh S. European Journal of Pharmaceutics and Biopharmaceutics Lipid – An emerging platform for oral delivery of drugs with poor bioavailability. Eur J Pharm Biopharm. 2009; 73: 1-15.
15. Weber S, Zimmer A, Pardeike J. European Journal of Pharmaceutics and Biopharmaceutics Solid Lipid Nanoparticles (SLN) and Nanostructured Lipid Carriers (NLC) for pulmonary application: A review of the state of the art. Eur J Pharm Biopharm. 2013.
16. Pham D, Fattal E, Tsapis N. Pulmonary drug delivery systems for tuberculosis treatment. Int J Pharm. 2015; 478: 517-529.
17. Hickey AJ. Back to the Future : Inhaled Drug Products. J Pharm Sci. 2013; 102: 1165-1172.
18. Mehnert W, Mader K. Solid lipid nanoparticles Production , characterization and applications. Adv Drug Deliv Rev. 2001; 47: 165-196.
19. Chono S, Tanino T, Seki T, Morimoto K. Uptake characteristics of liposomes by rat alveolar macrophages : influence of particle size and surface mannose modification. J Pharm Pharmcology. 2007; 59: 75-80.
20. Taylor P, Justo OR, Moraes ÂM, Moraes M. Incorporation of Antibiotics in Liposomes designed for Tuberculosis therapy by inhalation. Drug Deliv. 2015; 10: 201-207.
21. Pandey R, Sharma S, Khuller GK. Nebulization of liposome encapsulated antitubercular drugs in guinea pigs. Int J Antimicrob Agents. 2004; 24: 93-94.
22. Rojanarat W, Nakpheng T, Thawithong E, Yanyium N. Inhaled pyrazinamide proliposome for targeting alveolar macrophages. Drug Deliv. 2012; 19: 334-345.
23. Vyas SP, Kannan ME, Jain S, Mishra V, Singh P. Design of liposomal aerosols for improved delivery of rifampicin to alveolar macrophages. Int J Pharm. 2004; 269: 37-49.
24. Zaru M, Sinico C, Logu A De, et al. Rifampicin-loaded liposomes for the passive targeting to alveolar macrophages: *in vitro* and in vivo evaluation. J Liposome Res. 2009; 19: 68-76.
25. Chuan J, Li Y, Yang L. Enhanced rifampicin delivery to alveolar macrophages by solid lipid nanoparticles. J Nanoparticle Res. 2013; 15: 1634.
26. Pandey R, Sharma S, Khuller GKÃ. Oral solid lipid nanoparticle-based antitubercular chemotherapy. Tuberculosis. 2005; 85: 415-420.
27. Maretti E, Rossi T, Bondi M, et al. Inhaled Solid Lipid Microparticles to target alveolar macrophages for tuberculosis. Int J Pharm. 2014; 462: 74-82.
28. Vieira AC, Chaves LL, et al. Mannosylated solid lipid nanoparti-

cles for the selective delivery of rifampicin to macrophages. Artif Cells, Nanomedicine, Biotechnol. 2018: 1-11.

29. Witoonsaridsilp W, Paeratakul O, Panyarachun B, Sarisuta N. Development of Mannosylated Liposomes Using Synthesized N -Octadecyl- D - Mannopyranosylamine to Enhance Gastrointestinal Permeability for Protein Delivery. AAPS Pharm Sci Tech. 2012; 13: 699-706.

30. Tran TH, Ramasamy T, Truong DH, Choi H, Yong CS, Kim JO. Preparation and Characterization of Fenofibrate-Loaded Nanostructured Lipid Carriers for Oral Bioavailability Enhancement. AAPS Pharm Sci Tech. 2014; 15: 1509-1515.

31. Pilcer G, Amighi K. Formulation strategy and use of excipients in pulmonary drug delivery. Int J Pharm. 2010;392(1-2):1-19.

32. Mosmann T. Rapid Colorimetric Assay for Cellular Growth and Survival : Application to Proliferation and Cytotoxicity Assays. J Immunological Methods. 1983; 65: 55-63.

33. Ingh SS, Obhal AKD, Ain AJ, Andit JKP. Formulation and Evaluation of Solid Lipid Nanoparticles of a Water Soluble Drug : Zidovudine. Chem Pharm Bull. 2010; 58: 650-655.

34. Alves R, Vitória T, Carlos L, Storpírtis S, Mercuri P, Matos R. Thermal behavior and decomposition kinetics of rifampicin polymorphs under isothermal and non-isothermal conditions. Brazilian J Pharm Sci. 2010; 46: 343-351.

35. Aboutaleb E, Noori M, Gandomi N, Atyabi F, Fazeli MR. Improved antimycobacterial activity of rifampin using solid lipid nanoparticles. Int Nano Lett. 2012; 2: 33.

36. Mulla JAS, Mabrouk M, Choonara YE, et al. Development of respirable rifampicin-loaded nano-lipomer composites by microemulsion- spray drying for pulmonary delivery. J Drug Deliv Sci Technol. 2017; 41: 13-19.

37. Parumasivam T, Yoon R, Chang K, et al. Dry powder inhalable formulations for anti-tubercular therapy. Adv Drug Deliv Rev. 2016; 102: 83-101.

38. Dey A, Chatterji D. Tracing the Variation in Physiological Response to Rifampicin Across the Microbial Spectrum. J Bacteriol Virol. 2012; 42: 87-100.

39. Bemer-melchior P, Bryskier A, Drugeon HB. Comparison of the in vitro activities of rifapentine and rifampicin against Mycobacterium tuberculosis complex. J Antimicrob Chemother. 2000; 46: 571-575.

40. Greenspan P, Mayer EP, Fowler SD. Nile Red " A Selective Fluorescent Stain for Intracellular Lipid Droplets. J Cell Biol. 1985; 100: 965-973.

41. Takenaga M, Ohta Y, Tokura Y, Hamaguchi A, Igarashi R. Lipid Microsphere Formulation Containing Rifampicin Targets Alveolar Macrophages. Drug Deliv. 2008; 15: 169-175.